Available online at www.sciencedirect.com
ScienceDirect
International Journal of Heat and Mass Transfer 50 (2007) 4927–4936
International Journal of HEAT and MASS TRANSFER
www.elsevier.com/locate/ijhmt

Combined forced and free flow in a vertical circular duct subjected to non-axisymmetric wall heating conditions

A. Barletta *, S. Lazzari

Dipartimento di Ingegneria Energetica, Nucleare e del Controllo Ambientale (DIENCA), Università di Bologna, Via dei Colli 16, I-40136 Bologna, Italy

Received 21 August 2006
Available online 7 June 2007

Abstract

The fully developed mixed convection flow in a vertical circular duct is investigated analytically, under the assumption of laminar parallel flow. A wall heat flux uniform in the axial direction and dependent on the angular coordinate is considered. As a consequence, the fluid temperature is three dimensional, since it changes in the radial, axial and angular directions. An analytical method based on Fourier series expansions of temperature and velocity fields is adopted to determine the velocity and the temperature distributions as well as the friction factor and the average Nusselt number. The general solution, expressed in terms of Bessel functions, is applied to study a case that has a special importance in technical applications: a duct whose wall is half subject to a uniform heat flux and half adiabatic. The positive and negative threshold values of the ratio between the Grashof number *Gr* and the Reynolds number *Re* for the onset of the flow reversal phenomenon are determined. A comparison between the average Nusselt number for the considered non-axisymmetric case and that for the case of a duct subject to a uniform wall heat flux is performed.

Keywords: Non-axisymmetric boundary conditions; Circular duct; Mixed convection; Laminar flow; Analytical methods

1. Introduction

Laminar mixed convection in vertical or inclined circular ducts is a subject that has been extensively studied over the last decades. For instance, the review papers [1,2], as well as the references therein, show the most important results achieved on this subject. In fact, most papers on this topic refer to axisymmetric thermal boundary conditions. For example, in [3] the Author discussed the fully developed mixed convection in a vertical tube in the case of laminar flow with a uniform wall heat flux. However, there are several technical cases such that the wall temperature and the wall heat flux depend on the angular coordinate. Non-axisymmetric thermal boundary conditions have been studied, for instance, in [4] and, more recently, in [5]. In [6], the Authors studied the case of a horizontal duct with half cross-section subject to a uniform wall heat flux and the other half adiabatic.

In the present paper, mixed convection flow in a vertical circular duct is studied with reference to a wall heat flux which is uniform along the axial direction and is an arbitrary function of the angular coordinate. Therefore, a net fluid heating occurs in the flow direction. The fully developed region is studied and laminar parallel flow is considered. Moreover, the Boussinesq approximation is applied by assuming the axially varying average temperature in a duct section as the reference fluid temperature. As it has been shown in [7], this assumption is the best choice to ensure the validity of the Boussinesq approximation. The momentum and energy balance equations are written in a dimensionless form and are solved by employing an analytical method based on Fourier series expansions of both the temperature field and the velocity field with respect to the angular coordinate ϑ. The velocity field, the temperature field, the friction factor and the average Nusselt number are evaluated. A special case is studied in detail: the case

* Corresponding author.
E-mail address: antonio.barletta@mail.ing.unibo.it (A. Barletta).

0017-9310/$ - see front matter © 2007 Elsevier Ltd. All rights reserved.
doi:10.1016/j.ijheatmasstransfer.2007.03.039

Nomenclature

A	dimensionless parameter, defined by Eq. (24)
$b_0(r)$, $a_n(r)$, $b_n(r)$	Fourier series coefficients, employed in Eq. (20)
$h_0(r)$, $c_n(r)$, $h_n(r)$	Fourier series coefficients, employed in Eq. (21)
f	Fanning friction factor, defined by Eq. (54)
$F(\vartheta)$	dimensionless arbitrary function of ϑ, defined by Eq. (19)
$\mathbf{g}$	gravitational acceleration vector
g	magnitude of the gravitational acceleration
Gr	Grashof number, defined in Eq. (6)
I_n, J_n	Bessel functions of order n
k	thermal conductivity of the fluid
m,n	positive integers
$\overline{Nu}$	average Nusselt number, defined by Eq. (62)
$\overline{Nu}_{sym}$	average Nusselt number for uniform wall heat flux
P	difference between the pressure and the hydrostatic pressure
$q_w(\vartheta)$	local wall heat flux per unit area
$\overline{q}_w$	average value of q_w
r	dimensionless radial coordinate, defined in Eq. (6)
R	radial coordinate
R_0	radius of the duct
Re	Reynolds number, defined in Eq. (6)
t	dimensionless temperature, defined in Eq. (6)
t_b	dimensionless bulk temperature, defined by Eq. (60)
t_{peak}	peak value of the dimensionless temperature
$\overline{t}_w$	dimensionless average wall temperature, defined by Eq. (64)
T	temperature
T_b	bulk temperature of the fluid, defined by Eq. (59)
T_0	average fluid temperature in a duct section, defined by Eq. (7)
$\overline{T}_w$	average wall temperature
u	dimensionless velocity, defined in Eq. (6)
$\mathbf{U}$	fluid velocity vector
U	X-component of the fluid velocity
U_0	average velocity in a duct section, defined by Eq. (9)
W_n	function of A, defined by Eq. (45)
X	axial coordinate

Greek symbols

α	thermal diffusivity
β	volumetric coefficient of thermal expansion
γ_n	Fourier series coefficients, employed in Eq. (19)
ΔT	reference temperature difference
ϑ	angular coordinate
λ	dimensionless pressure drop, defined in Eq. (6)
Λ_1	positive threshold value of Gr/Re
Λ_2	negative threshold value of Gr/Re
μ	dynamic viscosity
ν	kinematic viscosity
ρ	mass density
ρ_0	mass density for $T = T_0$
$\overline{\tau}_w$	average wall shear stress, defined by Eq. (55)
ω_n	Fourier series coefficients, employed in Eq. (19)

of a vertical circular duct having a wall which is half subject to a uniform heat flux and half adiabatic. The solution shows that the velocity profile can be strongly influenced by the buoyancy forces and may display flow reversal phenomena. Plots of both the dimensionless temperature and the dimensionless velocity as functions of the angular coordinate ϑ and of the dimensionless radial coordinate r are presented for some values of the ratio between the Grashof number Gr and the Reynolds number Re. Moreover, an analysis of the conditions for the occurrence of the flow reversal phenomenon is performed and the positive and negative threshold values of Gr/Re are determined. Finally, the average Nusselt number is compared with that of a duct subject to a uniform axisymmetric wall heat flux.

2. Mathematical model

Let us consider a vertical circular duct with radius R_0 and a cylindrical coordinate system (X, R, ϑ), as sketched in Fig. 1. Let us suppose that a Newtonian fluid flows

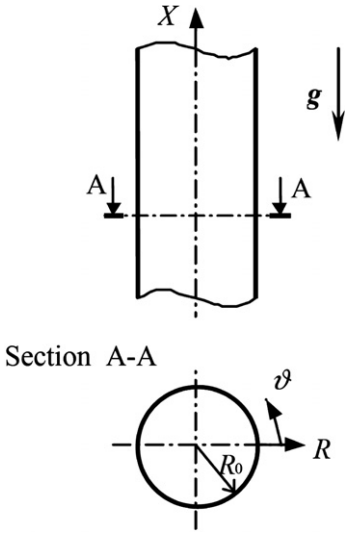

Fig. 1. The vertical circular duct and the cylindrical coordinate system.

inside the duct in fully developed steady laminar regime. The flow is assumed to be parallel, so that the velocity vector **U** has the only non-vanishing component U along the X-axis. Moreover, the effect of viscous dissipation is considered as negligible.

The thermal boundary conditions considered are such that the wall heat flux is both axially uniform and an arbitrary function of the angular coordinate ϑ. Therefore, in general, a net fluid heating occurs in the flow direction, so that $\partial T/\partial X \neq 0$.

Let us invoke the Boussinesq approximation with a linear equation of state, namely

$$\rho = \rho_0[1 - \beta(T - T_0)], \tag{1}$$

where T_0 is the average temperature on a duct cross-section. As a consequence, **U** results in a solenoidal field and, therefore,

$$\partial U/\partial X = 0. \tag{2}$$

Let us consider the case of a duct subject to an incoming wall heat flux that is an arbitrary function of ϑ:

$$q_w(\vartheta) = k \left.\frac{\partial T}{\partial R}\right|_{R=R_0} = \overline{q}_w F(\vartheta), \tag{3}$$

where the average value $\overline{q}_w$ on the circumference is given by

$$\overline{q}_w = \frac{k}{2\pi}\int_0^{2\pi} d\vartheta \left.\frac{\partial T}{\partial R}\right|_{R=R_0}. \tag{4}$$

By means of Eqs. (3) and (4), one can conclude that the average value of the arbitrary function $F(\vartheta)$ on the circumference must be equal to 1, i.e.

$$\frac{1}{2\pi}\int_0^{2\pi} d\vartheta F(\vartheta) = 1. \tag{5}$$

Let us define the dimensionless quantities

$$t = \frac{T - T_0}{\Delta T}, \quad u = \frac{U}{U_0}, \quad r = \frac{R}{R_0}, \quad \lambda = -\frac{4R_0^2}{\mu U_0}\frac{dP}{dX}, \quad Re = \frac{2R_0U_0}{\nu}, \quad Gr = \frac{8g\beta\Delta T R_0^3}{\nu^2}, \quad \frac{Gr}{Re} = \frac{4g\beta\Delta T R_0^2}{\nu U_0} \tag{6}$$

and let us assume the following reference temperature T_0, reference temperature difference ΔT and reference velocity U_0,

$$T_0 = \frac{1}{\pi R_0^2}\int_0^{2\pi} d\vartheta \int_0^{R_0} dR\, R T(X, R, \vartheta), \tag{7}$$

$$\Delta T = \frac{2R_0\overline{q}_w}{k}, \tag{8}$$

$$U_0 = \frac{1}{\pi R_0^2}\int_0^{2\pi} d\vartheta \int_0^{R_0} dR\, R U(R, \vartheta). \tag{9}$$

On account of Eqs. (6) and (8), positive values of Gr/Re can be obtained for upward flow when the duct is heated as well as for downward flow when the duct is cooled. On the other hand, negative values of Gr/Re can be obtained for upward flow when the duct is cooled as well as for downward flow when the duct is heated.

In the fully developed regime, the quantity dP/dX is a constant. Moreover,

$$\frac{\partial T}{\partial X} = \frac{dT_0}{dX} = \frac{d\overline{T}_w}{dX} = \frac{2\alpha\overline{q}_w}{kR_0U_0}, \tag{10}$$

where

$$\overline{T}_w(X) = \frac{1}{2\pi}\int_0^{2\pi} d\vartheta\, T(X, R_0, \vartheta) \tag{11}$$

is the average wall temperature. Therefore, one has

$$t = t(r, \vartheta). \tag{12}$$

By means of Eqs. (6), (8) and (10), the momentum balance equation in the X-direction and the energy balance equation can be written in the following dimensionless form, respectively:

$$\frac{1}{r}\frac{\partial}{\partial r}\left(r\frac{\partial u}{\partial r}\right) + \frac{1}{r^2}\frac{\partial^2 u}{\partial \vartheta^2} + \frac{1}{4}\frac{Gr}{Re}t + \frac{\lambda}{4} = 0, \tag{13}$$

$$\frac{1}{r}\frac{\partial}{\partial r}\left(r\frac{\partial t}{\partial r}\right) + \frac{1}{r^2}\frac{\partial^2 t}{\partial \vartheta^2} - u = 0. \tag{14}$$

The no slip condition at the wall implies that

$$u(1, \vartheta) = 0. \tag{15}$$

Eqs. (3), (6) and (8) yield

$$\left.\frac{\partial t}{\partial r}\right|_{r=1} = \frac{1}{2}F(\vartheta). \tag{16}$$

Moreover, both the dimensionless velocity and the dimensionless temperature on the duct axis must be finite.

Finally, since T_0 and U_0 are the average values of T and U in a duct cross-section, the following constraints on the functions $t(r, \vartheta)$ and $u(r, \vartheta)$ hold:

$$\int_0^{2\pi} d\vartheta \int_0^1 dr\, rt = 0, \tag{17}$$

$$\int_0^{2\pi} d\vartheta \int_0^1 dr\, ru = \pi. \tag{18}$$

3. General solution of the balance equations

Under the assumption that the function $F(\vartheta)$ that appears in Eq. (5) is continuous for $0 \leqslant \vartheta \leqslant 2\pi$, it can be expressed as a Fourier series of sines and cosines, as follows:

$$F(\vartheta) = 1 + \sum_{n=1}^{\infty}[\gamma_n \sin(n\vartheta) + \omega_n \cos(n\vartheta)]. \tag{19}$$

Similarly, since the functions $t\,(r, \vartheta)$ and $u\,(r, \vartheta)$ are continuous for $0 \leqslant r \leqslant 1$ and $0 \leqslant \vartheta \leqslant 2\pi$, they can be expanded as Fourier series in the variable ϑ, as follows:

$$t(r,\vartheta)=\frac{b_0(r)}{2}+\sum_{n=1}^{\infty}[a_n(r)\sin(n\vartheta)+b_n(r)\cos(n\vartheta)], \tag{20}$$

$$u(r,\vartheta)=\frac{h_0(r)}{2}+\sum_{n=1}^{\infty}[c_n(r)\sin(n\vartheta)+h_n(r)\cos(n\vartheta)]. \tag{21}$$

On account of Eqs. (20) and (21), the dimensionless momentum balance equation (13) and the dimensionless energy balance equation (14) can be written respectively as

$$\frac{1}{2}\left[\frac{1}{r}\frac{\mathrm{d}}{\mathrm{d}r}\left(r\frac{\mathrm{d}h_0}{\mathrm{d}r}\right)-A^4b_0\right]+\frac{\lambda}{4}+\sum_{n=1}^{\infty}\left\{\left[\frac{1}{r}\frac{\mathrm{d}}{\mathrm{d}r}\left(r\frac{\mathrm{d}c_n}{\mathrm{d}r}\right)-\frac{n^2}{r^2}c_n-A^4a_n\right]\sin(n\vartheta)+\left[\frac{1}{r}\frac{\mathrm{d}}{\mathrm{d}r}\left(r\frac{\mathrm{d}h_n}{\mathrm{d}r}\right)-\frac{n^2}{r^2}h_n-A^4b_n\right]\cos(n\vartheta)\right\}=0, \tag{22}$$

$$\frac{1}{2}\left[\frac{1}{r}\frac{\mathrm{d}}{\mathrm{d}r}\left(r\frac{\mathrm{d}b_0}{\mathrm{d}r}\right)-h_0\right]+\sum_{n=1}^{\infty}\left\{\left[\frac{1}{r}\frac{\mathrm{d}}{\mathrm{d}r}\left(r\frac{\mathrm{d}a_n}{\mathrm{d}r}\right)-\frac{n^2}{r^2}a_n-c_n\right]\sin(n\vartheta)+\left[\frac{1}{r}\frac{\mathrm{d}}{\mathrm{d}r}\left(r\frac{\mathrm{d}b_n}{\mathrm{d}r}\right)-\frac{n^2}{r^2}b_n-h_n\right]\cos(n\vartheta)\right\}=0, \tag{23}$$

where

$$A^4=-\frac{1}{4}\frac{Gr}{Re}. \tag{24}$$

By means of Eqs. (19)–(21), the boundary conditions (15) and (16) and the constraints (17) and (18) yield, respectively,

$$\frac{h_0(1)}{2}+\sum_{n=1}^{\infty}[c_n(1)\sin(n\vartheta)+h_n(1)\cos(n\vartheta)]=0, \tag{25}$$

$$\frac{1}{2}\left.\frac{\mathrm{d}b_0}{\mathrm{d}r}\right|_{r=1}+\sum_{n=1}^{\infty}\left[\left.\frac{\mathrm{d}a_n}{\mathrm{d}r}\right|_{r=1}\sin(n\vartheta)+\left.\frac{\mathrm{d}b_n}{\mathrm{d}r}\right|_{r=1}\cos(n\vartheta)\right]=\frac{1}{2}\left\{1+\sum_{n=1}^{\infty}[\gamma_n\sin(n\vartheta)+\omega_n\cos(n\vartheta)]\right\}, \tag{26}$$

$$\int_0^1 \mathrm{d}r\, rb_0=0, \tag{27}$$

$$\int_0^1 \mathrm{d}r\, rh_0=1. \tag{28}$$

3.1. Determination of $b_0(r)$, $h_0(r)$ and λ

The functions $b_0(r)$, $h_0(r)$ and the parameter λ can be determined by solving the differential equations that can be obtained from Eqs. (22)–(28).

In detail, by integrating Eqs. (22), (23), (25) and (26) with respect to ϑ in the range $[0,2\pi]$, one obtains, respectively,

$$\frac{1}{r}\frac{\mathrm{d}}{\mathrm{d}r}\left(r\frac{\mathrm{d}h_0}{\mathrm{d}r}\right)-A^4b_0+\frac{\lambda}{2}=0, \tag{29}$$

$$\frac{1}{r}\frac{\mathrm{d}}{\mathrm{d}r}\left(r\frac{\mathrm{d}b_0}{\mathrm{d}r}\right)-h_0=0, \tag{30}$$

$$h_0(1)=0, \tag{31}$$

$$\left.\frac{\mathrm{d}b_0}{\mathrm{d}r}\right|_{r=1}=1. \tag{32}$$

On account of Eqs. (27)–(32), one has

$$h_0(r)=A\frac{J_0(A)I_0(Ar)-I_0(A)J_0(Ar)}{J_0(A)I_1(A)-I_0(A)J_1(A)}, \tag{33}$$

$$b_0(r)=\frac{J_0(A)[AI_0(Ar)-2I_1(A)]+I_0(A)[AJ_0(Ar)-2J_1(A)]}{A^2[J_0(A)I_1(A)-I_0(A)J_1(A)]}, \tag{34}$$

$$\lambda=4A^2\frac{I_1(A)J_0(A)+I_0(A)J_1(A)}{I_0(A)J_1(A)-J_0(A)I_1(A)}. \tag{35}$$

In the limit $Gr/Re\to 0$, i.e. when $A\to 0$, one obtains the solution in the forced convection regime. In this limit, Eqs. (33)–(35) yield

$$h_0(r)=4(1-r^2), \tag{36}$$

$$b_0(r)=-\frac{5}{12}+r^2-\frac{r^4}{4}, \tag{37}$$

$$\lambda=32. \tag{38}$$

3.2. Determination of $a_n(r)$ and $c_n(r)$

If one multiplies Eqs. (22), (23), (25) and (26) by $\sin(m\vartheta)$, where m is an arbitrary positive integer, and then integrates with respect to ϑ in the range $[0,2\pi]$, one obtains, respectively,

$$\frac{1}{r}\frac{\mathrm{d}}{\mathrm{d}r}\left(r\frac{\mathrm{d}c_n}{\mathrm{d}r}\right)-\frac{n^2}{r^2}c_n-A^4a_n=0, \tag{39}$$

$$\frac{1}{r}\frac{\mathrm{d}}{\mathrm{d}r}\left(r\frac{\mathrm{d}a_n}{\mathrm{d}r}\right)-\frac{n^2}{r^2}a_n-c_n=0, \tag{40}$$

$$c_n(1)=0, \tag{41}$$

$$\left.\frac{\mathrm{d}a_n}{\mathrm{d}r}\right|_{r=1}=\frac{\gamma_n}{2}. \tag{42}$$

On account of Eqs. (39)–(42), one has

$$c_n(r)=\frac{A\gamma_n[J_n(A)I_n(Ar)-I_n(A)J_n(Ar)]}{W_n(A)}, \tag{43}$$

$$a_n(r)=\frac{\gamma_n[J_n(A)I_n(Ar)+I_n(A)J_n(Ar)]}{AW_n(A)}, \tag{44}$$

where $W_n(A)$ is given by

$$W_n(A)=[I_{n-1}(A)+I_{n+1}(A)]J_n(A)+[J_{n-1}(A)-J_{n+1}(A)]I_n(A). \tag{45}$$

In the limit of forced convection ($A\to 0$), Eqs. (43) and (44) yield

$$c_n(r) = 0, \tag{46}$$

$$a_n(r) = \frac{\gamma_n r^n}{2n}. \tag{47}$$

3.3. Determination of $b_n(r)$ and $h_n(r)$

If one multiplies Eqs. (22), (23), (25) and (26) by $\cos(m\vartheta)$, where m is an arbitrary positive integer, and then integrates with respect to ϑ in the range $[0, 2\pi]$, one obtains, respectively,

$$\frac{1}{r}\frac{\mathrm{d}}{\mathrm{d}r}\left(r\frac{\mathrm{d}h_n}{\mathrm{d}r}\right) - \frac{n^2}{r^2}h_n - A^4 b_n = 0, \tag{48}$$

$$\frac{1}{r}\frac{\mathrm{d}}{\mathrm{d}r}\left(r\frac{\mathrm{d}b_n}{\mathrm{d}r}\right) - \frac{n^2}{r^2}b_n - h_n = 0, \tag{49}$$

$$h_n(1) = 0, \tag{50}$$

$$\left.\frac{\mathrm{d}b_n}{\mathrm{d}r}\right|_{r=1} = \frac{\omega_n}{2}. \tag{51}$$

By comparing Eqs. (48)–(51) with Eqs. (39)–(42), one obtains

$$h_n(r) = \frac{\omega_n}{\gamma_n}c_n(r), \tag{52}$$

$$b_n(r) = \frac{\omega_n}{\gamma_n}a_n(r). \tag{53}$$

For the particular case of a duct subject to a uniform wall heat flux which does not depend on the angular coordinate ϑ, i.e. for $F(\vartheta) = 1$, the dimensionless temperature field $t(r, \vartheta)$ and the dimensionless velocity field $u(r, \vartheta)$ coincide with $b_0(r)/2$ and $h_0(r)/2$, respectively, and agree with the expressions reported in [8]. Moreover, on account of Eqs. (36), (46) and (52), in the limit of forced convection ($A \to 0$), $u(r, \vartheta)$ tends to the dimensionless Poiseuille velocity profile.

3.4. Comments on the general solution

An important feature of the general solution arises from the denominators appearing in Eqs. (33)–(35), i.e. $J_0(A)I_1(A) - I_0(A)J_1(A)$, and in Eqs. (43) and (44), i.e. $W_n(A)$. When these denominators vanish, singularities of the solution may arise. It is well known that, in the axisymmetric wall heat flux case, when only the zero-order modes in the Fourier series expansions are involved, the singularity with the lowest absolute value of Gr/Re occurs for $Gr/Re = -1808.02$ [8]. This value of Gr/Re corresponds to a zero of $J_0(A)I_1(A) - I_0(A)J_1(A)$. In Refs. [3,7], it is pointed out that the physical significance of the first singularity occurring for $Gr/Re = -1808.02$ is the occurrence of unstable flow for $Gr/Re \leqslant -1808.02$. In fact, due to the singularity, in a neighborhood of $Gr/Re = -1808.02$, a small perturbation of the boundary conditions (value of $\bar{q}_w$) results in an arbitrarily large modification of the velocity and temperature profiles.

In the non-axisymmetric case, also the zeros of $W_n(A)$ for $n \geqslant 1$ must be considered. One observes that there is a zero of $W_1(A)$ for $Gr/Re = -271.849$. On the other hand, the quantities $W_n(A)$ for $n \geqslant 2$ present zeros for values of Gr/Re smaller than -1808.02. Therefore, by applying the same reasoning introduced by Morton [3] in the axisymmetric case, one can deduce that flow instabilities arise even for $Gr/Re \leqslant -271.849$ when the mixed convection is non-axisymmetric. More precisely, the occurrence of flow instabilities for $Gr/Re \leqslant -271.849$ applies to non-axisymmetric cases such that $\gamma_1 \neq 0$ and $\omega_1 \neq 0$. Thermal boundary conditions such that $\gamma_1 = 0 = \omega_1$ lead to instabilities for $Gr/Re \leqslant -1808.02$, i.e. in the same range defined for uniform wall heat flux. In the following, only flow regimes with $Gr/Re > -271.849$ will be considered.

4. Fanning friction factor, bulk temperature and Nusselt number

The Fanning friction factor f is defined as

$$f = \frac{\bar{\tau}_w}{\frac{1}{2}\rho_0 U_0^2}, \tag{54}$$

where $\bar{\tau}_w$ is the average wall shear stress given by

$$\bar{\tau}_w = -\frac{\mu}{2\pi}\int_0^{2\pi}\mathrm{d}\vartheta \left.\frac{\partial U}{\partial R}\right|_{R=R_0}. \tag{55}$$

By means of Eqs. (6) and (55), Eq. (54) yields

$$f = -\frac{2}{\pi}\frac{1}{Re}\int_0^{2\pi}\mathrm{d}\vartheta \left.\frac{\partial u}{\partial r}\right|_{r=1}. \tag{56}$$

By integrating Eq. (13) on the duct cross-section and by employing Eq. (17) together with the Gauss–Green theorem, one obtains

$$\lambda\pi + 4\int_0^{2\pi}\mathrm{d}\vartheta \left.\frac{\partial u}{\partial r}\right|_{r=1} = 0. \tag{57}$$

As a consequence,

$$f\,Re = \frac{\lambda}{2}. \tag{58}$$

Hence, from Eq. (38), in the limit of forced convection, one obtains $f\,Re = 16$.

Since the bulk temperature T_b is defined as

$$T_b = \frac{1}{\pi R_0^2 U_0}\int_0^{2\pi}\mathrm{d}\vartheta\int_0^{R_0}\mathrm{d}R\,RUT, \tag{59}$$

the dimensionless bulk temperature is given by

$$t_b = \frac{T_b - T_0}{\Delta T} = \frac{1}{\pi}\int_0^{2\pi}\mathrm{d}\vartheta\int_0^1 \mathrm{d}r\,rut. \tag{60}$$

Eq. (60) shows that the dimensionless quantity t_b is invariant along the axial direction. By employing Eqs. (20), (21), (33), (34), (43), (44), (52) and (53), one obtains

$$t_b = -\frac{(A^2+4)J_0(A)^2 I_1(A)^2 + (A^2-4)I_0(A)^2 J_1(A)^2}{4A^2[J_0(A)I_1(A) - I_0(A)J_1(A)]^2} + \frac{1}{2}\sum_{n=1}^{\infty}\frac{\gamma_n^2+\omega_n^2}{W_n(A)^2}[I_n(A)^2 J_{n-1}(A)J_{n+1}(A) - J_n(A)^2 I_{n-1}(A)I_{n+1}(A)]. \quad (61)$$

With reference to an arbitrary cross-section of the duct, the average Nusselt number is given by

$$\overline{Nu} = \frac{2R_0}{k}\frac{\bar{q}_w}{\overline{T}_w - T_b}. \quad (62)$$

On account of Eqs. (6), (8) and (60), one obtains

$$\overline{Nu} = \frac{1}{\bar{t}_w - t_b}, \quad (63)$$

where $\bar{t}_w$ is the dimensionless average wall temperature, defined as

$$\bar{t}_w = \frac{\overline{T}_w - T_0}{\Delta T} = \frac{1}{2\pi}\int_0^{2\pi} d\vartheta\ t(1,\vartheta). \quad (64)$$

By means of Eqs. (20), (34), (44) and (53), one obtains

$$\bar{t}_w = \frac{1}{A^2}\left[1 + \frac{AJ_0(A)I_2(A)}{J_0(A)I_1(A) - I_0(A)J_1(A)}\right]. \quad (65)$$

In the limit of forced convection ($A \to 0$), one obtains

$$\bar{t}_w = \frac{1}{6}, \quad t_b = -\frac{1}{16}, \quad \overline{Nu} = \frac{48}{11} \quad (66)$$

for any possible assignment of $F(\vartheta)$.

5. Technical application: duct with partially insulated wall

With reference to Fig. 2, let us consider a case of technical interest. In detail, let us assume that the duct is subject to a uniform wall heat flux for $0 < \vartheta < \pi$ and is adiabatic for $\pi < \vartheta < 2\pi$. On account of Eqs. (5) and (19), the function $F(\vartheta)$ can be expressed as a Fourier series of sines only, as follows:

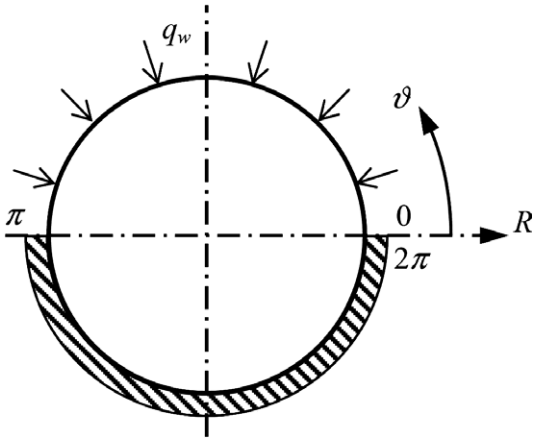

Fig. 2. Duct with partially insulated wall.

$$F(\vartheta) = 1 + \sum_{n=1}^{\infty}\gamma_n \sin(n\vartheta), \quad (67)$$

where

$$\gamma_n = \frac{4}{\pi n} \quad \text{for } n \text{ odd}, \qquad \gamma_n = 0 \quad \text{for } n \text{ even}. \quad (68)$$

Since the coefficients ω_n are zero, Eqs. (52) and (53) reveal that, in this case,

$$h_n(r) = b_n(r) = 0. \quad (69)$$

By noticing that $\gamma_1 \neq 0$, one can conclude that the range of validity of the solution is $Gr/Re > -271.849$, as it can be inferred from the discussion presented in Section 3.4.

On account of Eqs. (43), (44) and (68), one obtains

$$c_{2n-1}(r) = \frac{4A[J_{2n-1}(A)I_{2n-1}(Ar) - I_{2n-1}(A)J_{2n-1}(Ar)]}{\pi(2n-1)W_{2n-1}(A)}, \quad (70)$$

$$a_{2n-1}(r) = \frac{4[J_{2n-1}(A)I_{2n-1}(Ar) + I_{2n-1}(A)J_{2n-1}(Ar)]}{\pi(2n-1)AW_{2n-1}(A)}, \quad (71)$$

$$c_{2n}(r) = a_{2n}(r) = 0. \quad (72)$$

Eqs. (61), (67) and (68) yield

$$t_b = -\frac{(A^2+4)J_0(A)^2 I_1(A)^2 + (A^2-4)I_0(A)^2 J_1(A)^2}{4A^2[J_0(A)I_1(A) - I_0(A)J_1(A)]^2} + \frac{8}{\pi^2}\sum_{n=1}^{\infty}\frac{1}{(2n-1)^2 W_{2n-1}(A)^2} \times [I_{2n-1}(A)^2 J_{2(n-1)}(A)J_{2n}(A) - J_{2n-1}(A)^2 I_{2(n-1)}(A)I_{2n}(A)]. \quad (73)$$

It is easily shown that there exists a positive real number Λ_1 such that flow reversal occurs for $Gr/Re > \Lambda_1 > 0$. Indeed, for $Gr/Re = \Lambda_1$, the first derivative of $u(r,\vartheta)$ with respect to r evaluated for $r = 1$ and $\vartheta = 3\pi/2$ vanishes. On account of Eqs. (21), (33) and (69)–(72), one obtains

$$\Lambda_1 = 359.503. \quad (74)$$

On the other hand, there exists a negative real number Λ_2 such that flow reversal occurs for $Gr/Re < \Lambda_2 < 0$. Indeed, for $Gr/Re = \Lambda_2$, the first derivative of $u(r,\vartheta)$ with respect to r evaluated for $r = 1$ and $\vartheta = \pi/2$ vanishes. On account of Eqs. (21), (33) and (69)–(72), one obtains

$$\Lambda_2 = -69.0175. \quad (75)$$

One can observe that the loss of axial symmetry in the thermal boundary conditions leads to a non-symmetric behavior in the onset of the flow reversal phenomenon, i.e. $\Lambda_1 \neq -\Lambda_2$.

The analytical solution can be used to perform a detailed study of the temperature and velocity distribution in this technical case. To obtain results either in tabular or graphical form, one must truncate the infinite Fourier series to a finite number of terms sufficient to reach a prescribed accuracy. In order to test the accuracy of the truncated Fourier series, a comparison has been made with a finite-element 2D solution of the governing equations

Table 1
Values of $\overline{Nu}$ and $\overline{Nu}_{sym}$ versus Gr/Re

Gr/Re	$\overline{Nu}$		$\overline{Nu}_{sym}$		
	Analytical	Numerical	Analytical	Numerical	Ref. [9]
−271.849	0	0.0000000	3.60686	3.60676	–
−250	0.0245445	0.0245449	3.67021	3.67021	–
−200	0.306888	0.306889	3.81361	3.81361	–
−150	0.965788	0.965790	3.95473	3.95473	–
−100	1.97169	1.97170	4.09348	4.09348	–
−50	3.16933	3.16934	4.22980	4.22980	–
0	48/11	4.36364	48/11	4.36364	–
100	6.27957	6.27957	4.62371	4.62371	–
200	7.48724	7.48724	4.87356	4.87356	–
300	8.23252	8.23251	5.11324	5.11323	–
400	8.73030	8.73029	5.34290	5.34289	5.03
500	9.09958	9.09957	5.56280	5.56280	5.34
600	9.40011	9.40010	5.77328	5.77328	5.61
700	9.66179	9.66178	5.97472	5.97471	5.85
800	9.89992	9.89990	6.16750	6.16750	6.06
900	10.1226	10.1226	6.35206	6.35205	6.26
1000	10.3342	10.3342	6.52880	6.52880	6.44

(13)–(18). The latter solution has been obtained by means of software Comsol Multiphysics (© Comsol, Inc.). The mesh adopted is unstructured and has 3048 elements. Table 1 reports values of $\overline{Nu}$ and $\overline{Nu}_{sym}$. The quantity $\overline{Nu}_{sym}$ is the average Nusselt number for a duct subject to an axisymmetric uniform wall heat flux. Since, in the axisymmetric case, one has $\gamma_n = \omega_n = 0$, $\overline{Nu}_{sym}$ can be easily evaluated from Eq. (63), with $\bar{t}_w$ given by Eq. (65) and t_b expressed as

$$t_b = -\frac{(A^2+4)J_0(A)^2 I_1(A)^2 + (A^2-4)I_0(A)^2 J_1(A)^2}{4A^2[J_0(A)I_1(A) - I_0(A)J_1(A)]^2}. \quad (76)$$

Table 1 displays values obtained either by the analytical Fourier series solution truncated to the first 50 terms or by the numerical finite-element solution. Values of Gr/Re not less than −271.849 are considered in Table 1, as well as in Table 2, following the criterion specified in Subsection 3.4. The last column of Table 1 contains the values of $\overline{Nu}_{sym}$ obtained by the correlation

$$\overline{Nu}_{sym} = 0.9973\left(\frac{Gr}{Re}\right)^{0.27}, \quad 4\times 10^2 \leqslant \frac{Gr}{Re} \leqslant 4\times 10^4 \quad (77)$$

reported in Hallman [9]. Table 1 reveals an almost perfect agreement within 6 digits accuracy between the average Nusselt number evaluated analytically and numerically, both in the non-axisymmetric case and in the axisymmetric case. The comparison with the values of $\overline{Nu}_{sym}$ obtained through Hallman's correlation (77) yields a relative error that decreases with Gr/Re from about 6% for $Gr/Re = 400$ to about 1.5% for $Gr/Re = 1000$. In fact, as specified in Eq. (77), Hallman's correlation is designed to fit the data in a range of values of Gr/Re only marginally overlapping with that considered in Table 1. In Table 2, values of λ and of the peak dimensionless temperature t_{peak} are reported. The peak dimensionless temperature is the maximum value of the dimensionless temperature t in the duct. Inspection of the thermal boundary conditions leads one to conclude that the condition $t = t_{peak}$ occurs in the position $r = 1$ and $\vartheta = \pi/2$, i.e. in the central position of the isoflux half boundary. Table 2 shows a comparison between the values of λ and t_{peak} obtained analytically and numerically. The values of t_{peak} obtained analytically require Fourier series truncated to the first 500 terms in order to ensure six digits accuracy. Since, as specified in Subsection 3.4, the value $Gr/Re = -271.849$ corresponds to a singularity of the temperature field, the quantity t_{peak} becomes infinite for this value of Gr/Re. The comparison between values of λ and t_{peak} obtained analytically and numerically reveals a very good agreement. It must be pointed out that the discrepancy between the data of λ becomes slightly higher only for $Gr/Re = -271.849$ due to the peculiarity of this limiting case. Table 3 contains an illustration of

Table 2
Values of λ and t_{peak} versus Gr/Re

Gr/Re	λ		t_{peak}	
	Analytical	Numerical	Analytical	Numerical
−271.849	12.7366	12.5601	–	–
−250	14.4792	14.4793	5.87287	5.87269
−200	18.3237	18.3237	2.00374	2.00370
−150	21.9829	21.9829	1.30753	1.30752
−100	25.4728	25.4728	1.01487	1.01487
−50	28.8076	28.8076	0.852987	0.852989
0	32	32.0000	0.749788	0.749794
100	38.0012	38.0012	0.624917	0.624927
200	43.5532	43.5532	0.551337	0.551350
300	48.7183	48.7183	0.502294	0.502310
400	53.5474	53.5474	0.466940	0.466957
500	58.0829	58.0829	0.440032	0.440050
600	62.3600	62.3600	0.418723	0.418742
700	66.4083	66.4083	0.401329	0.401350
800	70.2529	70.2529	0.386789	0.386811
900	73.9154	73.9153	0.374401	0.374424
1000	77.4140	77.4140	0.363679	0.363702

Table 3
Series convergence check of the value of $\overline{Nu}$ for $Gr/Re = 1000$

No. of terms	$\overline{Nu}$
1	10.19291927
6	10.33420096
11	10.33422760
16	10.33422835
21	10.33422843
26	10.33422844
31	10.33422844
36	10.33422845
41	10.33422845

the sensitivity of the analytically determined $\overline{Nu}$ to the number of terms adopted in the truncated Fourier series. Reference has been made to $Gr/Re = 1000$. Table 3 shows that the evaluation of $\overline{Nu}$ requires only 16 terms to attain eight digits accuracy. On the other hand, the convergence of the series involved in the evaluation of other quantities, as for instance the peak dimensionless temperature t_{peak}, is much slower.

In Figs. 3 and 4, the dimensionless temperature distribution and the dimensionless velocity distribution are plotted as functions of the angular coordinate ϑ, for $r = 0.5$ and for $Gr/Re = -100$, 0, 100, 1000. Fig. 3 shows that, both for positive and for negative values of Gr/Re, the dimensionless temperature t is always higher in the duct half where non-vanishing wall heat flux is prescribed ($0 \leqslant \vartheta \leqslant \pi$). This result does not, in general, imply that the fluid is hotter in the duct half $0 \leqslant \vartheta \leqslant \pi$. In fact, t has been obtained dividing the temperature difference $T - T_0$ by the constant ΔT proportional to $\bar{q}_w$ (Eq. (8)). Then, if $\bar{q}_w > 0$, the fluid is heated and, in the duct half $0 \leqslant \vartheta \leqslant \pi$, the temperature is higher than in the duct half $\pi < \vartheta < 2\pi$. On the other hand, if $\bar{q}_w < 0$, the fluid is cooled and, in the duct half $0 \leqslant \vartheta \leqslant \pi$, the temperature is smaller than in the duct half $\pi < \vartheta < 2\pi$. This feature is not affected by the direction of flow (upward, $U_0 > 0$, or downward, $U_0 < 0$). In other words, the behavior of the distribution of t is not affected by the sign of Gr/Re, as it has been pointed out above. Fig. 4 displays the behavior of the dimensionless velocity distribution. Unlike for the dimensionless temperature, the sign of Gr/Re is important for the dimensionless velocity. Physically, the sign of Gr/Re determines whether buoyancy acts on the fluid in the same direction or in the opposite direction of the average flow. More precisely, when $Gr/Re > 0$, the fluid next to the isoflux half wall ($0 \leqslant \vartheta \leqslant \pi$) is subject to a buoyancy force directed as the average flow. The reverse occurs when $Gr/Re < 0$. This behavior can be recovered by inspecting the dimensionless velocity plots in Fig. 4. The plot of u corresponding to $Gr/Re = 1000$ reveals that a region of reversed flow ($u < 0$) arises next to the adiabatic wall.

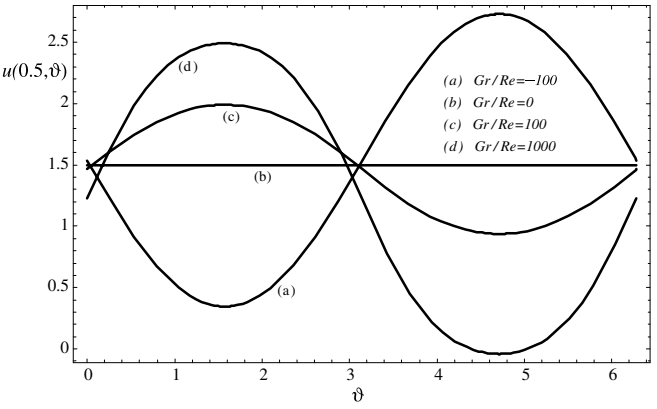

Fig. 4. Dimensionless velocity distributions for $r = 0.5$.

In Figs. 5 and 6, the dimensionless temperature distribution and the dimensionless velocity distribution are plotted as functions of the radial coordinate r on the vertical plane defined by $\vartheta = \pi/2$ and $\vartheta = 3\pi/2$, for $Gr/Re = -100$, 0, 100, 1000. For the same physical reasoning stated while commenting Fig. 3, the dimensionless temperature plots reported in Fig. 5 show that the maximum value of dimensionless temperature is obtained in correspondence of the isoflux half wall ($0 \leqslant \vartheta \leqslant \pi$). Fig. 6 shows that, for $Gr/Re = -100$ and $Gr/Re = 1000$, flow reversal phenomena arise, as expected from the threshold values of Gr/Re given in Eqs. (74) and (75).

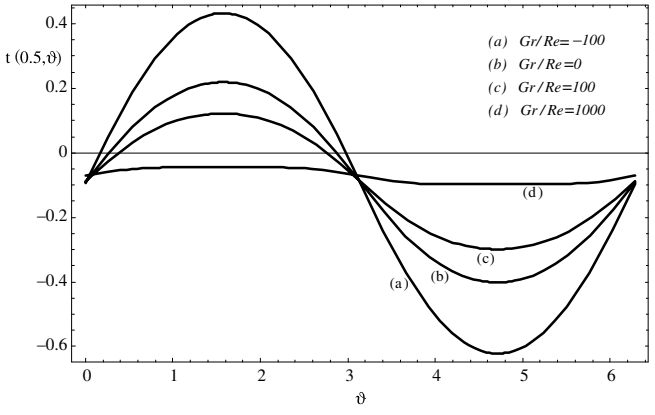

Fig. 3. Dimensionless temperature distributions for $r = 0.5$.

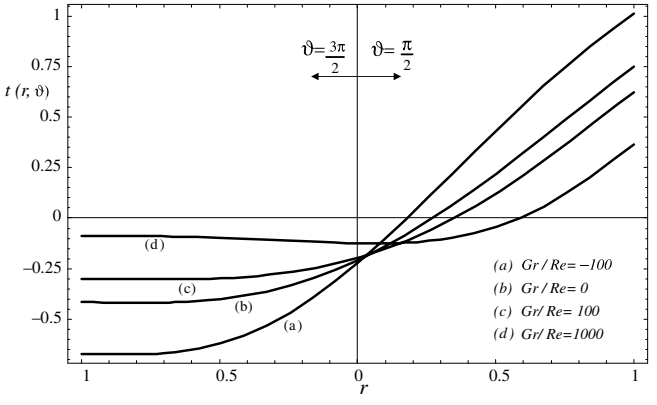

Fig. 5. Dimensionless temperature distributions on the plane $\vartheta = \pi/2$ and $\vartheta = 3\pi/2$.

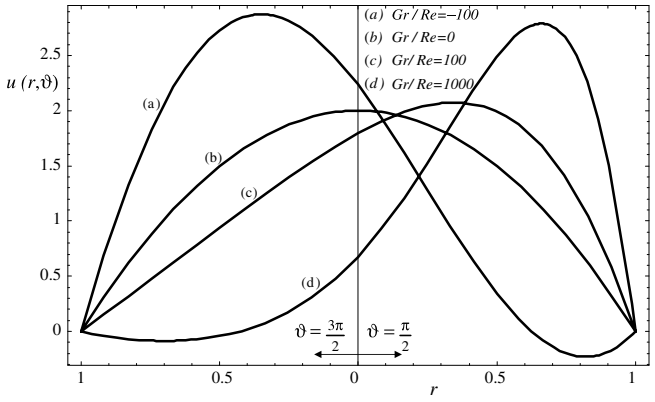

Fig. 6. Dimensionless velocity distributions on the plane $\vartheta = \pi/2$ and $\vartheta = 3\pi/2$.

In Figs. 7 and 8, the dimensionless temperature distribution $t(r,\vartheta)$ and the dimensionless velocity distribution $u(r,\vartheta)$ are represented for $Gr/Re = 1000$. In particular, Fig. 8 shows that, for this value of Gr/Re, strong deformations of the Poiseuille dimensionless velocity distribution

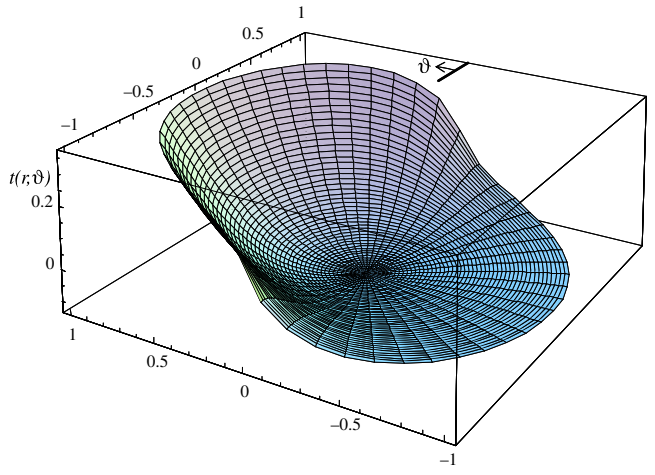

Fig. 7. Dimensionless temperature distribution for $Gr/Re = 1000$.

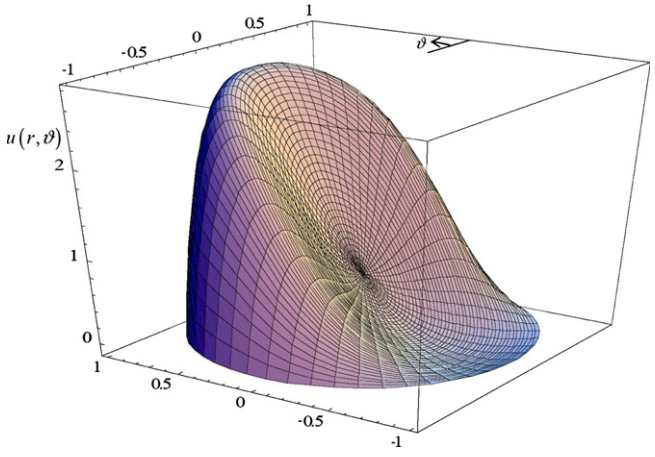

Fig. 8. Dimensionless velocity distribution for $Gr/Re = 1000$.

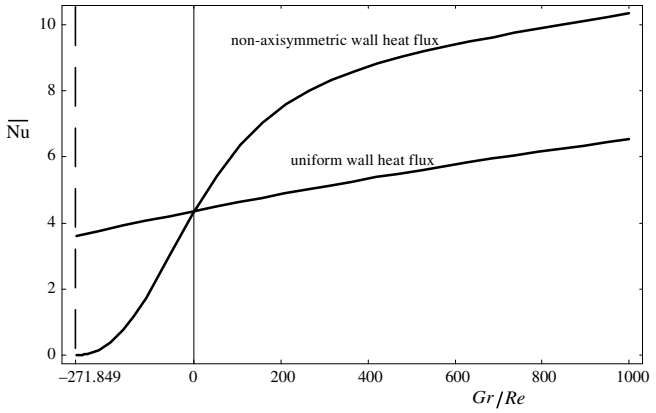

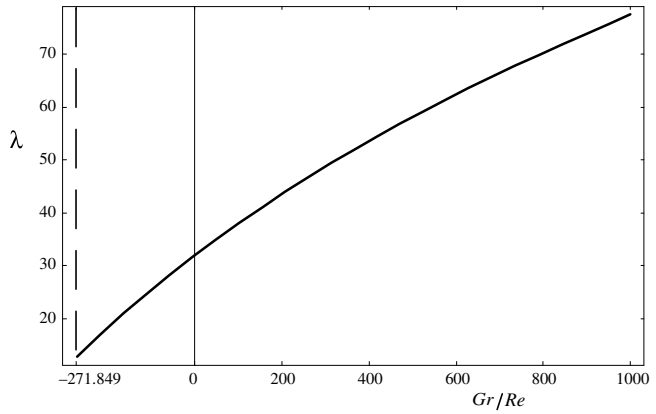

Fig. 9. Plots of $\overline{Nu}$ and λ versus Gr/Re for axisymmetric and non-axisymmetric wall heat flux.

occur. Namely, values of u higher than 2 can take place for $0 < \vartheta < \pi$, while negative values of u are present in the other half of the duct (flow reversal).

In Fig. 9, a comparison between the average Nusselt number $\overline{Nu}$ and the average Nusselt number $\overline{Nu}_{sym}$ relative to a duct subject to an axisymmetric uniform wall heat flux is presented. One can observe that in the limiting case of forced convection, i.e. for $Gr/Re = 0$, non-axisymmetric and axisymmetric thermal boundary conditions yield the same result, i.e. the well-known value 48/11. In Fig. 9, the plot of λ as a function of Gr/Re is also displayed. This plot shows that λ is an increasing function of Gr/Re. In other words, for a fixed average velocity U_0, buoyancy yields an increase of $|dP/dZ|$ when $Gr/Re > 0$. The reverse occurs for $Gr/Re < 0$.

6. Conclusions

The fully developed laminar mixed convection in a vertical circular duct has been studied in the case of thermal boundary conditions that are axially uniform and non-axisymmetric. An analytical solution of the dimensionless momentum and energy balance equations has been determined. Expressions of the dimensionless temperature field, of the dimensionless velocity field, of the dimensionless

bulk temperature and of the average Nusselt number have been provided.

A special case has been studied in detail: the case of a duct with half wall subject to a uniform heat flux and the other half adiabatic. The following results have been obtained.

- The buoyancy forces affect the dimensionless temperature field, the dimensionless velocity field, the dimensionless pressure drop parameter, the Fanning friction factor and the average Nusselt number.
- The positive and negative threshold values of Gr/Re for the onset of flow reversal have been determined. A lack of symmetry between the onset of flow reversal for upward flow and downward flow is induced by the non-axisymmetric thermal boundary conditions.
- The non-axisymmetric distribution of the wall heat flux influences significantly the value of the circumferentially averaged Nusselt number.

Appendix. How to obtain dimensional quantities

The results presented here have been determined in a dimensionless form. However, in practice, prediction of the values of dimensional quantities is the ultimate task. Typically, one may want to know the value of a given quantity, say the peak temperature, at a given axial station where the average fluid temperature T_0 has a known value. In fact, $T_0(X)$ is easily obtained for prescribed $\bar{q}_w$ and U_0 by integrating Eq. (10).

Let us assume that the fluid is heated, i.e. $\bar{q}_w > 0$, so that the maximum temperature occurs, for a given X, at $R = R_0$ and $\vartheta = \pi/2$. One evaluates Gr/Re on account of Eq. (6) by substituting the values of the thermophysical properties at temperature $T = T_0$. Then, from Table 2, one reads the value of t_{peak}. Finally, one evaluates the peak temperature as $T_0 + t_{peak}\Delta T$. The evaluated ratio Gr/Re can be also used, through Table 2, to determine λ and then obtain dP/dX as $-\lambda\mu U_0/(4R_0^2)$.

References

[1] W. Aung, Mixed convection in internal flow, in: Handbook of Single-Phase Convective Heat Transfer, John Wiley and Sons, New York, 1987 (Chapter 15).
[2] J.D. Jackson, M.A. Cotton, B.P. Axcell, Studies of mixed convection in vertical tubes, Int. J. Heat Fluid Flow 10 (1989) 2–15.
[3] B.R. Morton, Laminar convection in uniformly heated vertical pipes, J. Fluid Mech. 8 (1960) 227–240.
[4] W.C. Reynolds, Heat transfer to fully developed laminar flow in a circular tube with arbitrary circumferential heat flux, ASME J. Heat Transfer 82 (1960) 108–112.
[5] D.K. Choi, D.H. Choi, Developing mixed convection flow in a horizontal tube under circumferentially non-uniform heating, Int. J. Heat Mass Transfer 37 (1994) 1899–1913.
[6] S.V. Patankar, S. Ramadhyani, E.M. Sparrow, Effect of circumferentially nonuniform heating on laminar combined convection in a horizontal tube, ASME J. Heat Transfer 100 (1978) 63–70.
[7] A. Barletta, E. Zanchini, On the choice of the reference temperature for fully-developed mixed convection in a vertical channel, Int. J. Heat Mass Transfer 42 (1999) 3169–3181.
[8] A. Barletta, E. Rossi di Schio, Effect of viscous dissipation on mixed convection heat transfer in a vertical tube with uniform wall heat flux, Heat Mass Transfer 38 (2001) 129–140.
[9] T.M. Hallman, Combined forced and free laminar heat transfer in vertical tubes with uniform heat generation, ASME Trans. 78 (1956) 1831–1841.